Impedance Model of Eccentric Coil-Target Arrangements in Eddy Current Techniques

Dipl.-Ing. (FH) Jens Weidenmüller[1], M.Sc. Maral Heidary Dastjerdi[1], Prof. Dr. Jörg Himmel[1], Prof. Dr. Olfa Kanoun[2]

[1]Hochschule Ruhr West, Institut Mess- und Sensortechnik, 45473 Mülheim an der Ruhr
[2]Technische Universität Chemnitz, Fakultät für Elektrotechnik und Informationstechnik, 09111 Chemnitz

Abstract

Eddy current techniques are successfully applied over a wide application field in NDT (Non Destructive Testing), such as measurement of position, displacement, vibration, proximity and alignment. Nevertheless, this technology is not established for monitoring tasks in hot rolling mills. A desired application is the mass flow control of the semi-finished product (rod) during the rolling process. Between the rolling stands, the cross-sectional geometry (x-y plane) of the rod and its speed (z-axis) are of interest. A difficulty for the measurement is the changing x-y position (lateral offset) of the rod due to vibrations and the loose guidance in hot rolling mills.[1,2,3]
This contribution describes an analytic eddy current model which considers rod offsets (in x-y plane) for a static encircling coil (eddy current sensor element). The model is based on the TREE method (truncated region eigenfunction expansion) and can be used for coil design, selection of test frequencies and interpretation of the inspection data. In comparison to finite element analysis the described model allows a fast optimization of system parameters.
The paper is subdivided into five parts. After a short introduction a simplified circuit diagram of the setup illustrates the approach. Subsequently, the analytic model is introduced. This model yields the coil impedance in air (Z_0 gained from the well-established Dodd and Deeds models) and, in particular, the impedance change (ΔZ) produced by the eddy currents in the rod. Then the analytical findings will be compared with the experimental results. A final discussion concludes the paper in the last section.

Equivalent Circuit Diagramm

The eddy current measurement principle can be described with the air core transformer model [4]. The workpiece passes the encircling coil along the z-axis with varying x-y position inside the measuring section (fig.4). This arrangement is typical for monitoring tasks in hot rolling processes.

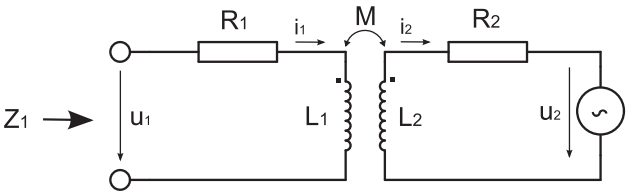

Figure 1 Equivalent coil-rod circuit diagram

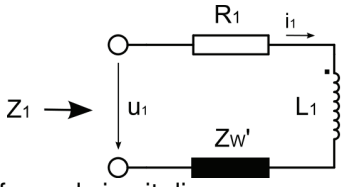

Figure 2 Transformed circuit diagram

In figure 1 the workpiece (rod) is considered as hot-wired secondary part, where R_2 and L_2 are the equivalent resistance and self-inductance of it depending on the eddy current path $i_2(t)$, conductivity σ and permeability μ. If the rod is located in the vicinity of the detection coil, both parts are coupled through the superposed electromagnetic fields. In common circuit diagrams the coupling between L_1 and L_2 is referred to as mutual inductance M. In the next step the complex impedance of the rod is transformed to the primary part (fig.2), as in consequence of the setup the complex impedance spectrum $Z_1=Z_{w'}+Z_{R1}+Z_{L1}$ is the measurand.

$$Z_1 = R_1 + \frac{\omega^2 M^2 R_2}{R_2^2 + \omega^2 L_2^2} + j\omega\left(L_1 - \frac{\omega^2 M^2 L_2}{R_2^2 + \omega^2 L_2^2}\right) \tag{1}$$

This equation clarifies that the detected impedance Z_1 changes corresponding to a different coil-rod coupling, where M depends on the rod's x-y position, its cross sectional area and its shape. In typical arrangements the path in which the eddy currents flow is centrically to the exciting current loop, as illustrated in figure 3. In this case, the mutual inductance M reads:

$$M = \frac{\phi_{12}}{I_1} = \frac{\phi_{21}}{I_2} = \frac{\mu_0}{4\pi} \oint_{C_2} \oint_{C_1} \frac{dl_1 dl_2}{\zeta_{12}} = \frac{\mu_0}{4\pi} \oint_{C_2} dl_2 \oint_{C_1} \frac{r_1 \cos(\beta)}{\sqrt{z^2 + r_1^2 + r_2^2 - 2r_1 r_2 \cos(\beta)}} d\beta \tag{2}$$

where β is the angle between source and target point (σ-φ) and the other parameters are stated in figure 3. Due to the symmetry and the even function in the numerator the integration can be performed analytically. Therefore equation 2 is transposed into a form with complete elliptic integrals of the first (K) and second (E) kinds [5]:

$$M = \mu_0 \frac{2r_1 r_2}{\sqrt{z^2 + (r_1 + r_2)^2}} \left[\left(\frac{2}{k^2} - 1 \right) K(k^2) - \left(\frac{2}{k^2} \right) E(k^2) \right] \tag{3}$$

with:

$$K(k^2) = \int_0^{\pi/2} \frac{1}{1 - k^2 \sin^2(\beta)} d\beta \quad ; \quad E(k^2) = \int_0^{\pi/2} 1 - k^2 \sin^2(\beta) d\beta \quad ; \quad k^2 = \frac{4r_1 r_2}{z_2 + (r_1 + r_2)^2} \tag{4}$$

These special integrals are tabulated and efficient numerical solutions are readily available in many standard mathematics software packages such as MATLAB©. If the rod moves out of centre position, the integration along the conductor loop can still be solved analytically but the one along the rod raises difficulties. For non-symmetric setups the description turns into a three-dimensional (3D) eddy current problem.

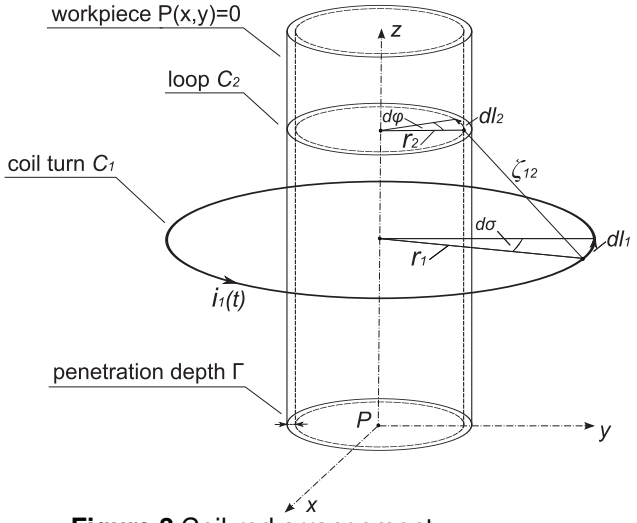

Figure 3 Coil-rod arrangement

Analytical Model

In this section we focus on the calculation of the coil impedance Z_1, the quantity of interest in eddy current testing. The complex impedance Z_1 can be expressed as the sum of the coil impedance in free space Z_0 and the impedance change ΔZ due to the presence of the conductive rod.

$$Z_1 = Z_0 + \Delta Z \tag{5}$$

The impedance Z_0 can be calculated with the well-established Dodd and Deed model that is used in eddy current non-destructive evaluation. In this model a multi-turn coil with round insulated-wire is approximated with a current sheet and the electromagnetic field is obtained by superposition. The impedance Z_0 reads in case of axial symmetry:

$$Z_0 = j\omega L_0 = \frac{j\omega 2\pi}{I} \frac{N}{cross - sectional\ area} \iint_{cross-sectional\ area} r A_\varphi dr dz \tag{6}$$

where ω is the angular frequency, N the coil wire turns, I the excitation current and A_φ is the sole component of the magnetic vector potential. If the rod is not located in the vicinity of the coil, the impedance Z_0 can be calculated as follows [6]:

$$Z_0 = \frac{j\omega 2\pi \mu_0 N^2}{(r_2 - r_1)^2 (z_2 - z_1)^2} \int_0^\infty \frac{\chi^2(\kappa r_1, \kappa r_2)}{\kappa^6} \left[\kappa(z_2 - z_1) + e^{-\kappa(z_2 - z_1)} - 1 \right] d\kappa \tag{7}$$

where the term $\chi(\kappa r_1, \kappa r_2)$ denotes a finite integral of the Bessel function that can be expressed with [7]:

$$\chi(x_1, x_2) = \int_{x_1}^{x_2} xJ_1(x)\,dx = \frac{\pi}{2} x[K_0(x)L_1(x) + K_1(x)L_0(x)]_{x_1}^{x_2} \tag{8}$$

This finite integral can be solved in a number of ways. The use of the modified Struve function (L_n) of order n and the modified Bessel function of the second kind (K_n) and order n is one possibility to calculate $\chi(\kappa r_1, \kappa r_2)$ efficiently.

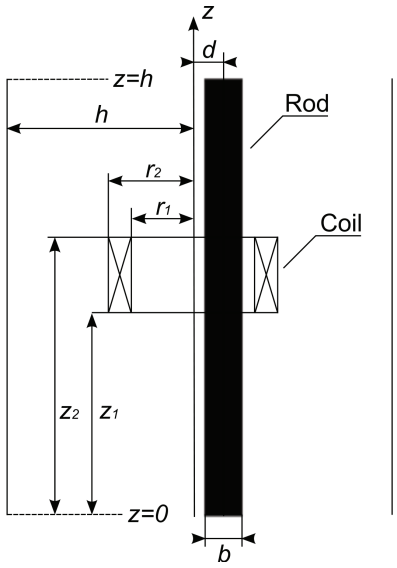

Figure 4 Static encircling coil around rod with lateral offset

The change of the impedance ΔZ due to the presence of a rod is calculated with the truncation region eigenfunction expansion (TREE) method. It differs from classic analytical forms in truncating the solution domain that would otherwise have an infinite range. As advantage the solution can be expressed as a series form, rather than as an integral. Also the class of problems that can be treated analytically is greatly extended. For example the arrangement in figure 4 can be calculated using this method. A detailed description of this method is given in [6]. The impedance change ΔZ for the give problem reads:

$$\Delta Z = \frac{j\omega 4\mu_0 N^2}{(r_2 - r_1)^2 (z_2 - z_1)^2} \frac{\pi}{h} \sum_{n=1}^{Ni} \sum_{m=0}^{Nm} (C\kappa^2 \cdot R) \cdot C \quad d\kappa \tag{9}$$

where the discrete eigenvalues κ_n of the problem are calculated from:

$$\kappa_n = \frac{n\pi}{h} \tag{10}$$

and C, R, M_{ub}, L_{ub} and L_{pb}:

$$C = \chi(\kappa r_1, \kappa r_2) \frac{\cos(\kappa z_2) - \cos(\kappa z_1)}{\kappa^4} \tag{11}$$

$$R = (2 - \delta_m) I_m(ud) \frac{I_m(ud)}{J_m(ud)} \cdot \frac{j\omega\mu_0\sigma \cdot m^2 + b^2 + p^2 u \cdot L_{pb} \cdot (-p \cdot L_{ub} + u \cdot L_{pb})}{j\omega\mu_0\sigma \cdot m^2 + b^2 + p^2 u \cdot L_{pb} \cdot (-p \cdot M_{ub} + u \cdot L_{pb})} \tag{12}$$

$$M_{ub} = \frac{m}{\kappa b} - \frac{K_{m+1}(\kappa b)}{K_m(\kappa b)}; \qquad L_{ub} = \frac{m}{\kappa b} + \frac{I_{m+1}(\kappa b)}{I_m(\kappa b)}; \qquad L_{pb} = \frac{m}{pb} - \frac{K_{m+1}(pb)}{K_m(pb)} \tag{13}$$

where δ_m is the Kronecker delta and $\chi(\kappa r_1, \kappa r_2)$ can also be calculated with equation 8. The variables I_m *and* K_m are the modified Bessel function of first kind and of second kind respectively. For the specific truncation length $h=40r_2$ the number of summation is set to *Ni=200* and *Nm=10.*

Experimental setup and results

In this section the analytical approach is compared with the corresponding experimental results to gain more information about the model. The results are achieved using two different coil geometries. Additionally the rod diameter and the offset position are swept within the region of interest. Those test parameters (listed bellow in table 1) are chosen to adapt the sensor behind the last rolling stand in a wire rolling mill. Figure 6 displays the engineering drawing of the prototype.
The laboratory test equipment consists of a stepper motor and control unit, mounting equipment and a PC with the control and read out software. In detail the positioning of the rod was made with a modular LNR Stage 50 mm ballscrew stepper motor (DRV114 0.05 µm resolution) and controlled via the software package LabView©. Figure 5 shows a photograph of this arrangement. The two investigated coil geometries differ considerably in the length, type I has a length of 63.5 mm and type II is shortened to 28 mm. During the parameter sweep the complex coil impedance was recorded with the laboratory impedance analyzer Agilent 4294.

coil	type I	type II
r_1 [mm]	12.5	12.5
r_2 [mm]	13.5	13.5
z_2-z_1 [mm]	63.5	28.0
wire diameter [mm]	1.0	1.0
turns	22	22
h [mm] (truncation domain)	$40r_2$	$40r_2$
msec [mm] (radius of measuring section within the coil)	5.5	5.5

rod	min	value	max	step
b [mm]	5		9	1
d [mm]	0		*msec*-b/2	(*msec*-b/2)/5
σ [MSm]		10.02		

excitation signal	
current amplitude	0.2 mA
frequency range	1-30 MHz
waveform	sinusoidal

Table 1 Test parameter

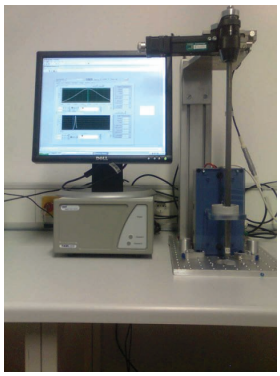

Figure 5 Laboratory setup

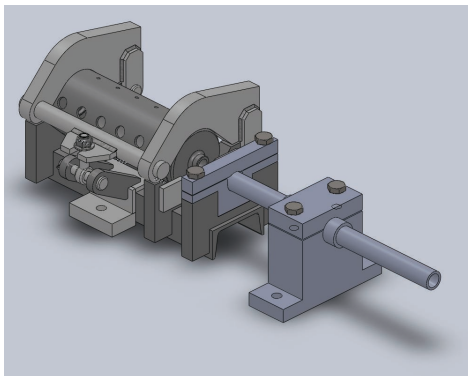

Figure 6 Mounting/shielding/guidance of the prototype

Typically the impedance plane, reactance vs. resistance, is selected in eddy current testing (ECT) to illustrate the measured data. The ECT is a multi-parametric method, where it is often necessary to separate the effect from different parameters that are varying at the same time. In this application the parameters are the desired cross-sectional area and the superimposed rod offset. Within the impedance plane we can see the effect of varying parameters in the reactance and resistance within a single plot. The achieved impedance planes for coil type I and II are shown in figure 7 and 8 respectively. The analytical model show comparable results in the reactance but it cannot follow the changes in resistance. This occurs since this part is neglected in equation 7. Nevertheless, the reactance is the quantity of interest in this application. Hence the read out frequency (3 MHz) is selected to minimize the effect of the undesired rod offset to the reactance, as shown in figure 7b and 8b. The maximum relative deviation (compared to the measured value) in the reactance reads ε_{X0}=2.27%. The notation ε_{X0} stands for the error in the reactance of Z_0 and ε_{X7mm} for the error in the reactance of ΔZ (rod diameter 7mm). The results are summarized in table 2.

	type I		type II	
	Z_0 [Ω] (ε_{X0})	Z_{7mm} [Ω] (ε_{X7mm})	Z_0 [Ω] (ε_{X0})	Z_{7mm} [Ω] (ε_{X7mm})
experiment	0.406+77.797i	1.876+74.352i	0.819+149.241i	3.489+142.405i
theory	0.000+79.565i (2,27%)	0.135+73.760i (0,80%)	0.000+147.792i (0,97%)	0.216+141.310i (0,79%)

Table 2 Comparison between experimental results and theory

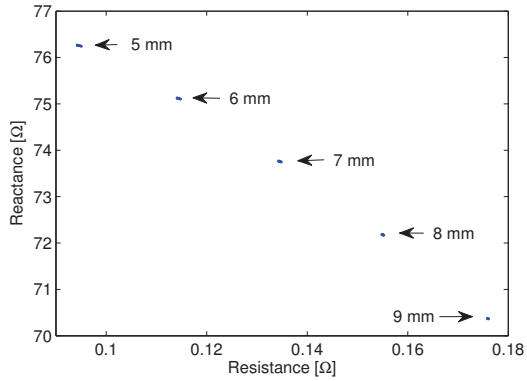

a) Analytical results at 3 MHz

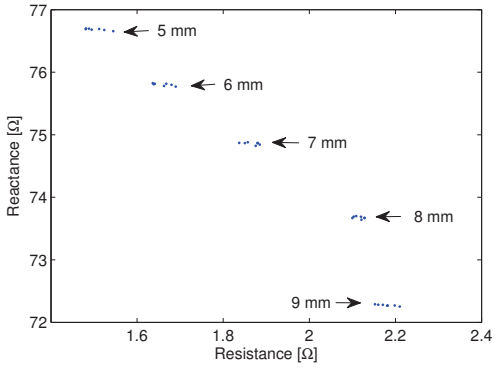

b) Measured results at 3 MHz

Figure 7 Impedance plane of different rod diameters swept within the measuring section (type I)

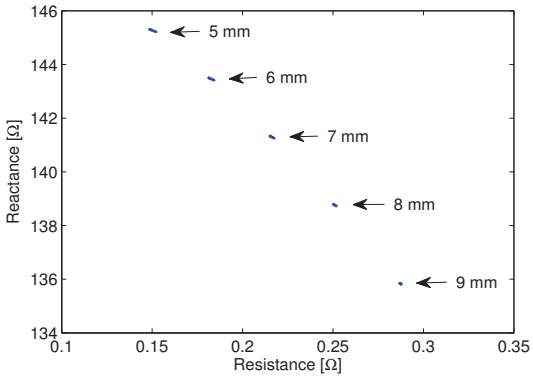

a) Analytical results at 3 MHz

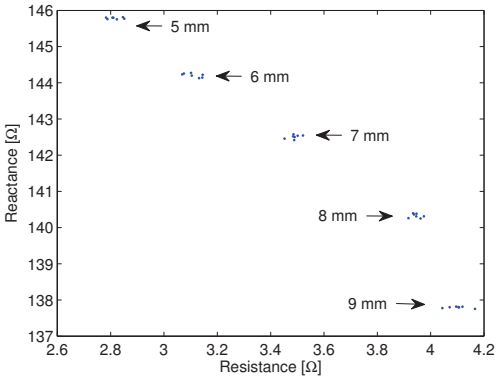

b) Measured results at 3 MHz

Figure 8 Impedance plane of different rod diameters swept within the measuring section (type I)

The influence of the rod offset to the coil reactance is clarified in the following plots (fig.9). Applying the selected operating frequency the reactance is heavily effected by the cross-sectional area of the rod. On the other hand rod offsets up to 3 mm within the measuring section effect the reactance only few mΩ. Table 3 shows the minimum resolution of both coils. As a result, the resolution of type I is almost twice compared to the shortened coil type II. This is due to crowing field inhomogeneities within the x-y plane (fig.3). The simulation results show the same trend with the advantage that the coil design can be characterized in a fraction of time. The elapsed time during the simulation was 6.29 s.

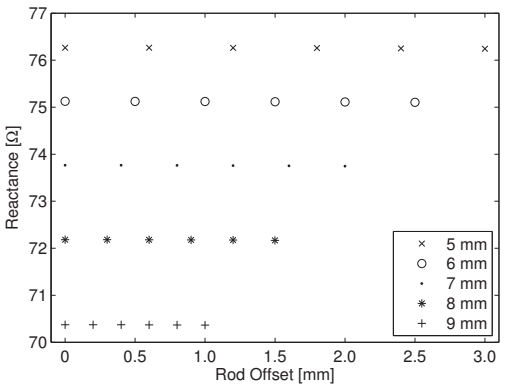

a) Analytical results at 3 MHz

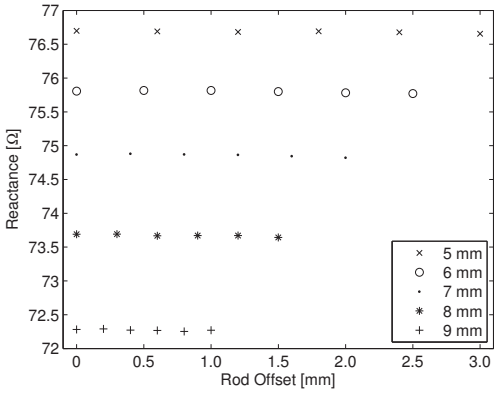

b) Measured results at 3 MHz

Figure 9 Reactance of different rod diameters swept within the measuring section (type I)

	type I		type II	
	resolution in Ø	resolution in *A*	resolution in Ø	resolution in *A*
experiment	55.56 µm	0.43 mm^2	88.34 µm	0.69 mm^2
theory	19.65 µm	0.15 mm^2	50.86 µm	0.40 mm^2

Table 3 minimum resolution in diameter Ø and cross-sectional area *A*

Conclusion

In hot rolling mills the semifinished product is subsequently reduced in size until the rod reaches the desired shape. In this process the rod passes up to 32 rolling sequences depending on the plant layout. If the mass flow of the semi finished product is continuous monitored in the meantime, the operating parameter could be readjusted at an early stage. This procedure contributes to achieve high quality standards.
Preliminary investigations illustrates that eddy current techniques stand out in this application. The resolution of ECT based sensors heavily depends on the filling factor (relation between rod and coil diameter). Hence an easy to use and fast method to fit the sensors to the plant layout is required. With the described analytical model the coil design and selection of test frequencies could be performed with 2.23% accuracy. The calculation time could be reduced to few seconds. This is the main advantage compared to finite element analyse (FEA) or experimental setups that are time-consuming. Due to the rod offset and resulting non-symmetrical arrangement the FEA must be performed in 3D. The required fine mesh due to the skin effect consideration increases the computational time rapidly.

Outlook

In the next step the model will be extended. The current model allows only round rod geometries but typical wearout failure in hot rolling mills lead to ovality defects. In this case it is promising to investigate the solution with elliptical coordinate system instead of the cylindrical.

References

[1] Himmel J., Knopf C., Schmüser I., Weidenmüller J., Wirbelstrombasierte Formmessung an metallischen Halbzeugen, Technisches Messen 1/2011, Oldenbourg Wissenschaftsverlag 2011.
[2] Himmel J., Arend S., Otto A., Sehestedt Ch., Produktionsflusskontrolle in Walzwerken mit elektromagnetischen Streufeldern, Sensoren Signale Systeme, Buchreihe Messen Prüfen Automatisieren, Bd. 6, b-Quadrat Verlag, Kreuztal 2006.
[3] Weidenmüller J., Knopf C., Sehestedt C., Himmel J., Rod Shape Testing by High Frequency Eddy Current – The experimental setup, I²MTC 2008 Conference IEEE IM Chapter, 14.05.2008 Vancouver Island,Verlag: IEEE Catalog Number: 08CH37941C Seite 1482-1486,
[4] Vyroubal D. Impedance of the Eddy-Current Displacement Probe: The Transformer Model, IEEE Transactions on Instrumentation and Measurement, Vol. 53, No. 2, April 2004.
[5] Gardiol F., Électromagnétisme - Traité d' Electricité, volume three. Presses Polytechniques et Universitaires Romandes, eight edition, 2004.
[6] Theodoulidis T. P., Kriezis E. E., Series expansions in eddy current nondestructive evaluation models, Elsavier Journal of Material Processing Technology 161 (2005) 343-347, 2006
[7] Theodoulidis T. P., Kriezis E. E., Eddy current canonical problems (with applications to nondestructive evaluation). Tech Science Press, 2006

Acknowledgment

My special thanks goes to Prof. Theodoros P. Theodoulidis who supported me programming the ΔZ formula.